Proceedings of 20th International Symposium on Music Acoustics
(Associated Meeting of the International Congress on Acoustics)

25-31 August 2010, Sydney and Katoomba, Australia

Refinements to the Model of a Single Woodwind Instrument Tonehole

Antoine Lefebvre and Gary P. Scavone

Computational Acoustic Modeling Laboratory (CAML)
Centre for Interdisciplinary Research in Music Media and Technology (CIRMMT)
Schulich School of Music of McGill University
555 Sherbrooke Street West, Montreal, QC H3A 1E3, Canada

PACS: 43.75.Ef,43.20.Mv

ABSTRACT

Using the Finite Element Method (FEM), a single unflanged tonehole was simulated for a wide range of heights and diameters in order to improve the accuracy of transmission-matrix calculations for instruments with toneholes of large diameter and short height, as found on saxophones and concert flutes. These calculations confirm the validity of existing models for toneholes of smaller diameter and longer height, as found on clarinets. Revised one-dimensional transmission-matrix models of open and closed toneholes are presented to extend the validity of the models based on the FEM results. Further, these tonehole models are verified to be valid for use with both cylindrical and conical (flare angles up to 6 degrees) air columns.

For open and closed toneholes, new formulas for the low frequency values of the shunt and series length correction are developed as a function of t/b and δ. Discrepancies with current theories are particularly apparent in the series length correction term. At higher frequencies, the open shunt equivalent length increases faster than previously predicted, corroborating recent experimental data (Dalmont et al., 2002). This effect is more important for short toneholes. These results do not take into account any possible internal or external interactions between the toneholes on an instrument, which may have an important effect for large-diameter toneholes.

INTRODUCTION

The design of a woodwind instrument using computer models requires precise calculations of the resonance frequencies of an air column with open and closed toneholes. Although there have been many theoretical, numerical, and experimental research studies on the single woodwind tonehole (Keefe 1982b; Keefe 1982a; Nederveen et al. 1998; Dubos et al. 1999a; Dalmont et al. 2002), it is known that current theories are not valid if the tonehole height t is shorter than the radius b (see Fig. 1) because "in that case the radiation field and the inner field are coupled" (Dalmont et al. 2002). Furthermore, the impact of the conicity of the main bore on the toneholes parameters has never been studied.

This paper describes improvements to the accuracy of transmission-matrix (TM) models of instruments with toneholes of large diameter and short height, as found on saxophones and concert flutes, obtained using the Finite Element Method (FEM). Current theoretical results from the literature are reviewed and the methodology with which we obtain the TM parameters from FEM simulations is presented. The FEM results are first validated with TM methods and with available experimental data. New results are presented that extend the validity of TM parameters for toneholes of dimensions used in most wind instruments. The main goal of this research is to obtain an accurate low frequency characterization of unflanged open and closed toneholes (up to 1 to 2 kHz).

THEORETICAL RESULTS

The TM representing a tonehole is defined as:

$$\mathbf{T}_{hole} = \begin{bmatrix} A & B \\ C & D \end{bmatrix}, \tag{1}$$

which, when inserted between two segments of cylindrical duct, relates the input and output quantities:

$$\begin{bmatrix} p_{in} \\ Z_0 U_{in} \end{bmatrix} = \mathbf{T}_{cyl}\mathbf{T}_{hole}\mathbf{T}_{cyl} \begin{bmatrix} p_{out} \\ Z_0 U_{out} \end{bmatrix}, \tag{2}$$

where $Z_0 = \rho c/S$ is the characteristic impedance of the waveguide, ρ is the density of air, c is the speed of sound in air and S is the cross-sectional area of the waveguide. The transmission matrix of a cylindrical duct of length L is:

$$\mathbf{T}_{cyl} = \begin{bmatrix} \cos kL & j\sin kL \\ j\sin kL & \cos kL \end{bmatrix}, \tag{3}$$

where $k = 2\pi f/c$ is the wavenumber and f is the frequency.

Based on the assumptions that $|\overline{Z}_a/\overline{Z}_s| \ll 1$ (Keefe 1982b, p. 677) and that the tonehole is symmetric, its TM may be approximated as a symmetric T section depending on two parameters, the shunt impedance $\overline{Z}_s = Z_s/Z_0$ and the series impedance $\overline{Z}_a = Z_a/Z_0$ (Keefe 1981), which becomes:

$$\begin{aligned} \mathbf{T}_{hole} &= \begin{bmatrix} 1 & \overline{Z}_a/2 \\ 0 & 1 \end{bmatrix} \begin{bmatrix} 1 & 0 \\ 1/\overline{Z}_s & 1 \end{bmatrix} \begin{bmatrix} 1 & \overline{Z}_a/2 \\ 0 & 1 \end{bmatrix} \\ &= \begin{bmatrix} 1+\frac{\overline{Z}_a}{2\overline{Z}_s} & \overline{Z}_a(1+\frac{\overline{Z}_a}{4\overline{Z}_s}) \\ 1/\overline{Z}_s & 1+\frac{\overline{Z}_a}{2\overline{Z}_s} \end{bmatrix}. \end{aligned} \tag{4}$$

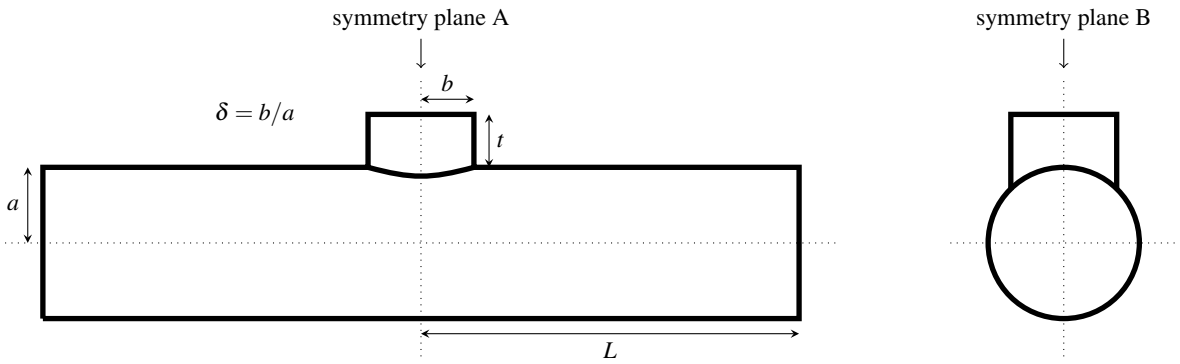

Figure 1: Diagram representing a tonehole on a cylindrical tube.

This equation was further simplified by Keefe, which replaces all occurrences of $\overline{Z}_a/\overline{Z}_s$ by zero, an approximation that introduces small but non-negligible errors in the calculation of the resonance frequencies.

The impedances $\overline{Z}_s$ and $\overline{Z}_a$ must be evaluated for the open (o) and closed (c) states of the tonehole as a function of geometry and frequency. Mathematical expressions for these impedances are available in the literature and are reviewed below.

Open Tonehole — Shunt Impedance

The open tonehole shunt impedance may be expressed as (Keefe 1982b):

$$\overline{Z}_s^{(o)} = jkt_s^{(o)} + \xi_s, \tag{5}$$

where ξ_s is the open tonehole shunt resistance and $t_s^{(o)}$ the tonehole equivalent length. The shunt resistance does not influence the calculated playing frequencies of a woodwind instrument and thus, most research efforts are concentrated on the determination of the shunt length correction. In the most recent literature (Dalmont et al. 2002), $t_s^{(o)}$ is written:

$$kt_s^{(o)} = kt_i + \tan k(t + t_m + t_r) \tag{6}$$

where t is the height of the tonehole as defined in Fig. 1, t_m is the matching volume equivalent length, t_r is the radiation length correction and t_i the inner length correction. Nederveen et al. (1998) obtained an accurate approximation for t_m:

$$t_m = \frac{b\delta}{8}\left(1 + 0.207\delta^3\right), \tag{7}$$

where $\delta = b/a$ is the ratio of the radius of the tonehole to the radius of the main bore.

The terms t_i and t_r are generally difficult to calculate analytically and, in the case where t is short, the coupling between the inner and outer length corrections prevents their separate analysis (Dalmont et al. 2002, sec. 2.7). The radiation length correction t_r depends on the external geometry; in the low frequency approximation, it may be that of a flanged pipe ($0.8216b$), an unflanged pipe ($0.6133b$) or another intermediary value for more complicated situations. The expressions provided in the literature for the inner length correction t_i are summarized in Table 2. These expressions are only valid for toneholes of large height ($t > b$). Note that there is an error in Eq. (5) of Dalmont et al. (2002), which refers to Eq. (55b) of Dubos et al. (1999a) — the correct version of this equation is reported here as Eq. 21.

In the limiting case where $t \to 0$ and $b \to 0$, the low-frequency characteristics of the tonehole are those of a hole in an infinitely thin wall (Pierce 1989, Eq. 7-5.10) and the total equivalent length of the hole becomes:

$$t_e = t + (\pi/2)b. \tag{8}$$

If the tonehole height is large but the radius $b \to 0$, the tonehole equivalent length becomes:

$$t_e = t + 0.6133b + 0.8216b = t + 1.4349b, \tag{9}$$

that is, the length of the tonehole with an unflanged length correction at the radiating end and a flanged radiation length correction inside the instrument.

The resistive term ξ_s influences the resonance magnitudes of an instrument but not their frequencies. In this paper, we focus on tuning considerations and thus do not consider this term further.

Open Tonehole — Series Impedance

The series impedance of the open tonehole is a small negative inertance:

$$\overline{Z}_a^{(o)} = jkt_a^{(o)}. \tag{10}$$

No significant resistive term was detected experimentally (Dalmont et al. 2002). Table 1 summarizes the equations found in the literature. In some publications, the exponent of δ is 2 whereas the results from our simulations as well as theoretical calculations by Keefe (1982b) show that the series length correction depends on δ^4. These equations were corrected in this paper.

Closed Tonehole — Shunt Impedance

The shunt impedance of a closed tonehole behaves mainly as a compliance (Nederveen 1998). This can be written:

$$\overline{Z}_s^{(c)} = -j\frac{1}{kt_s^{(c)}}. \tag{11}$$

The simplest expression for the shunt length correction is that of a closed cylinder of equivalent volume:

$$kt_s^{(c)} = \tan k(t + t_m). \tag{12}$$

An inner length correction may be considered as well for the closed tonehole but its influence is small relative to the cotangent term and becomes significant only at high frequencies (Keefe 1990). A recent expression including the inner length correction is (Nederveen et al. 1998, Eq. 7):

$$\overline{Z}_s^{(c)} = j\left[kt_i - \cot k(t + t_m)\right], \tag{13}$$

where t_i is the same as for the open tonehole as defined in Eq. 20.

Keefe 1982b, Eq. (68b)	$t_a^{(o)} = -\frac{0.47b\delta^4}{\tanh(1.84t/b)+0.62\delta^2+0.64\delta}$	(14)
Nederveen et al. 1998, Fig. 11	$t_a^{(o)} = -0.28b\delta^4$	(15)
Dubos et al. 1999a, Eq. (74)	$t_a^{(o)} = -\frac{b\delta^4}{1.78\tanh(1.84t/b)+0.940+0.540\delta+0.285\delta^2}$	(16)
Dubos et al. 1999a, not numbered	$t_a^{(o)} = -(0.37-0.087\delta)b\delta^4$	(17)

Table 1: Comparison of the expressions for the series length corrections $t_a^{(o)}$

Nederveen 1998, Eq. (38.3)	$t_i^{(o)} = (1.3-0.9\delta)b$	(18)
Keefe 1982b, Eq. (67a)	$t_i^{(o)} = (0.79-0.58\delta^2)b$	(19)
Nederveen et al. 1998, Eq. (40)	$t_i^{(o)} = (0.82-1.4\delta^2+0.75\delta^{2.7})b$	(20)
Dubos et al. 1999a, Eq. (73)	$t_i^{(o)} = t_s^{(o)} - t_a^{(o)}/4,$	(21)
	$t_s^{(o)} = (0.82-0.193\delta-1.09\delta^2+1.27\delta^3-0.71\delta^4)b$	

Table 2: Comparison of the expressions for the inner length correction $t_i^{(o)}$

Closed Tonehole — Series Impedance

The closed tonehole series impedance behaves as a small negative inertance, as for the open tonehole case. This can be expressed as:

$$\overline{Z}_a^{(c)} = jkt_a^{(c)}, \tag{22}$$

where $t_a^{(c)}$ is the series length correction. Keefe (1981, Eq. 54) proposed:

$$t_a^{(c)} = \frac{0.47b\delta^4}{\coth(1.84t/b)+0.62\delta^2+0.64\delta}, \tag{23}$$

whereas Dubos et al. (1999b, Eq. 74) calculated the length correction in the same situation as:

$$t_a^{(c)} = -\frac{b\delta^4}{1.78\coth(1.84t/b)+0.940+0.540\delta+0.285\delta^2}, \tag{24}$$

where we corrected the error in the exponent of δ (4 instead of 2).

INVESTIGATION METHOD

In this section, we present a method to calculate the transmission matrix $\mathbf{T}_{obj}$ of an object from the FEM. This method is useful to characterize an object that is part of a waveguide, i.e. which has an input and an output plane. It can be used to obtain the TM of any type of discontinuity in a waveguide. One requirement is that the evanescent modes occurring near the discontinuity must be sufficiently damped at the input and output planes of the simulated model. In general, cylindrical segments are thus required before and after a tonehole. The transmission matrix obtained from the simulations is given by $\mathbf{T} = \mathbf{T}_{cyl}\mathbf{T}_{obj}\mathbf{T}_{cyl}$ where the TM of a cylindrical duct was defined in Eq. 3. The effect of the cylinders is removed by calculation using the inverse of the cylinder's TM:

$$\mathbf{T}_{obj} = \mathbf{T}_{cyl}^{-1}\mathbf{T}\mathbf{T}_{cyl}^{-1}. \tag{25}$$

The object under study in this article being a tonehole with TM defined in Eqs. 1 and 4, we may extract the two impedances from the finite element simulation results with:

$$\overline{Z}_s = 1/C, \tag{26}$$

$$\overline{Z}_a = 2(A-1)/C. \tag{27}$$

A transmission matrix $\mathbf{T}$ contains four frequency-dependant complex-valued parameters relating input quantities to output quantities:

$$\begin{bmatrix} p_{in} \\ Z_0U_{in} \end{bmatrix} = \begin{bmatrix} T_{11} & T_{12} \\ T_{21} & T_{22} \end{bmatrix} \begin{bmatrix} p_{out} \\ Z_0U_{out} \end{bmatrix}. \tag{28}$$

In order to obtain these four parameters from finite element simulation results, we need to simulate the problem two times with different boundary conditions. By combining the results for the two simulation cases (subscript 1 and 2), we can write a system of linear equations to solve for the four parameters of the TM:

$$\begin{bmatrix} p_{out_1} & Z_0U_{out_1} & 0 & 0 \\ 0 & 0 & p_{out_1} & Z_0U_{out_1} \\ p_{out_2} & Z_0U_{out_2} & 0 & 0 \\ 0 & 0 & p_{out_2} & Z_0U_{out_2} \end{bmatrix} \begin{bmatrix} T_{11} \\ T_{12} \\ T_{21} \\ T_{22} \end{bmatrix} = \begin{bmatrix} p_{in_1} \\ Z_0U_{in_1} \\ p_{in_2} \\ Z_0U_{in_2} \end{bmatrix}. \tag{29}$$

The model of a tonehole on a cylindrical tube is symmetric (reversing the input and output conditions leads to the exact same system) and we take advantage of this feature to solve only one quarter of the geometry. One symmetry plane is perpendicular to the instrument body axis and is located on the center of the tonehole (A) whereas the second symmetry plane is defined by the axis of the instrument body and the axis of the tonehole (B) (see Fig. 1). On the second symmetry plane, the boundary condition is a null normal acceleration (symmetry). On the first symmetry plane we define alternatively a null normal acceleration for the symmetric case (case 1) and a null pressure for the anti-symmetric case (case 2). From the values of the pressure and normal velocity on the input plane of the model, we can deduce the values on the output plane for both simulation cases:

$$p_{out_1} = p_{in_1}, \tag{30}$$

$$Z_0U_{out_1} = -Z_0U_{in_1}, \tag{31}$$

$$p_{out_2} = -p_{in_2}, \tag{32}$$

$$Z_0U_{out_2} = Z_0U_{in_2}. \tag{33}$$

VALIDATION

The results of our simulations are compared with the experimental data obtained by Dalmont et al. (2002) and by Keefe (1982a). Dalmont et al. measured the shunt and series length corrections of a flanged tonehole as a function of frequency for two toneholes on a tube of radius a = 10 mm: (1) $\delta = 0.7$, $t/b = 1.3$ and (2) $\delta = 1.0$, $t/b = 1.01$. Both toneholes were flanged at their open end. We also compare our simulation results with data obtained by Keefe, who measured the shunt and series length corrections for two unflanged toneholes on a cylinder of radius a = 20 mm: (1) $\delta = 0.66$, $t/b = 0.48$ and (2) $\delta = 0.32$, $t/b = 3.15$.

The shunt length correction obtained from our simulations is displayed in Figs. 2 and 3 in comparison to the experimental results found in the literature. Our simulation results are in good general agreement with the experimental results of

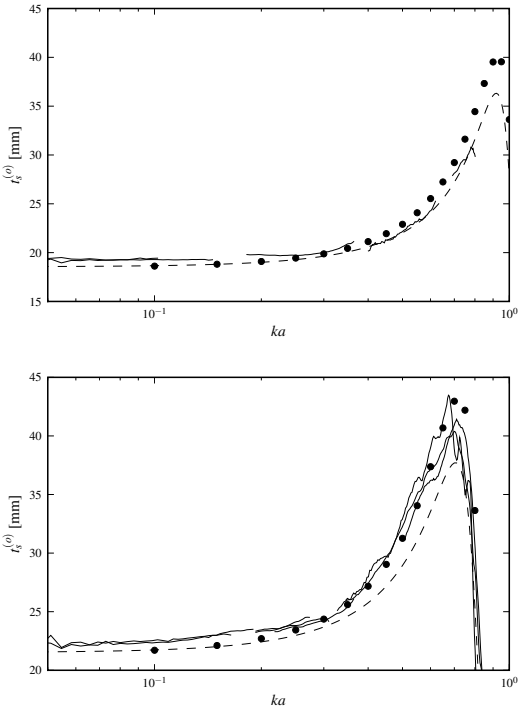

Figure 2: Shunt length correction $t_s^{(o)}$ as a function of ka for the two toneholes studied by Dalmont et al.: $\delta = 0.7$ and $t/b = 1.3$ (top graph), $\delta = 1.0$, $t/b = 1.01$ (bottom graph). FEM results (filled circles), experimental data from Dalmont et al. (solid lines) and theoretical results with Eq. 6 (dashed).

Dalmont et al. (2002) but a few interesting observation are worth mentioning: (1) the experimental data reveals a larger shunt length correction at low frequencies for both toneholes, compared to both the theoretical formula and our simulation results, which match; (2) the length correction predicted by our simulation results matches the experimental data for the larger diameter tonehole in the higher frequency range, predicting a larger length correction than the current theory.

In the case of the unflanged toneholes studied by Keefe (1982a), we found good agreement between the theoretical values, our simulations and his experimental data for the tonehole of tall height. For the short tonehole, there are discrepancies: the experimental data and our simulation results give larger length corrections for the higher frequencies compared to the theory.

For the results in Table 3, our FEM simulations for the smaller tonehole ($\delta = 0.7$) agree with the values predicted by the theoretical formulas but disagree with the experimental values obtained by Dalmont et al. (2002). In their article, Dalmont et al. (2002) used $t_a^{(o)} = -0.28b\delta^2$, in reference to an article by Nederveen et al. (1998), as a theoretical formula for the series length correction. As previously mentioned, we believe the series length correction varies as $b\delta^4$. And in fact, Dalmont et al. (2002) found a fairly high error with respect to that measurement. For the larger tonehole ($\delta = 1.0$), our simulations agree with the experimental data provided by Dalmont et al. (2002) and with all of the theoretical formulas except Eq. 14 from Keefe. The agreement with the results in Table 4 is satisfactory.

RESULTS AND DISCUSSION

The single open tonehole was simulated using the FEM for a wide range of geometric parameters ($\delta = b/a$ from 0.2 to 1.0 by step of 0.5, t/b from 0.1 to 0.3 by step of 0.05 and from 0.3

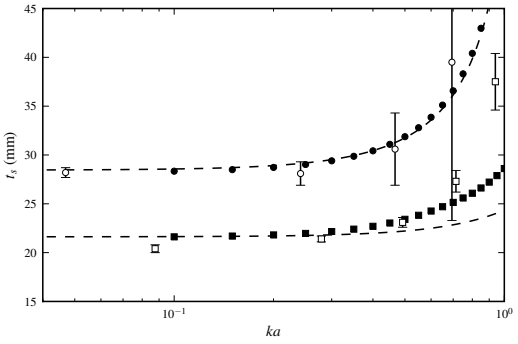

Figure 3: Shunt length correction $t_s^{(o)}$ as a function of ka for the two toneholes studies by Keefe: $\delta = 0.66$ and $t/b = 0.48$ (bottom curves), $\delta = 0.32$ and $t/b = 3.15$ (top curves). FEM results: for $\delta = 0.66$ (filled circles) and for $\delta = 0.32$ (filled squares). Experimental data from Keefe (markers with error bar) and theoretical results with Eq. 6 (dashed).

Tonehole			
δ	t/b	Description	$t_a^{(o)}$ [mm]
0.7	1.3	FEM	0.50
		Dalmont et al.	0.95±0.3
		Eq. 14	0.46
		Eq. 15	0.47
		Eq. 16	0.52
		Eq. 17	0.52
1.0	1.01	FEM	2.90
		Dalmont et al.	2.8±0.3
		Eq. 14	2.12
		Eq. 15	2.80
		Eq. 16	2.89
		Eq. 17	2.83

Table 3: Series length correction $t_a^{(o)}$ in mm. Comparison between simulation, theories, and experimental data for the toneholes studied by Dalmont et al.

to 1.3 by step of 0.2 and ka from 0.1 to 1.0 by step of 0.05 with an additional low frequency point at $ka = 0.01$). The lowest frequency simulated was 55 Hz. For each of these parameters, the four terms of the transmission matrix were obtained and the shunt and series length corrections calculated using the procedure previously described.

For the low frequency value of the shunt length correction (t_e), we were able to obtain a data-fit formula that matches the complete set of results. There is no data obtained for toneholes with $\delta < 0.2$ because, for such small-diameter toneholes, we were not able to obtain precise results. In order to ensure that the data-fit formula be valid for all values of δ, we added the two theoretical constraints expressed in Eqs. 8 and 9. The equation that we obtained is:

$$t_e/b = \lim_{k\to 0} t_s^{(o)}/b = t/b + [1 + f(\delta)g(\delta, t/b)]\,h(\delta), \quad (34)$$

with

$$f(\delta) = 0.095 - 0.422\delta + 1.168\delta^2 - 1.808\delta^3 + 1.398\delta^4 - 0.416\delta^5,$$

$$g(\delta, t/b) = 1 - \tanh(0.778\, t/b),$$

$$h(\delta) = 1.435 + 0.030\delta - 1.566\delta^2 + 2.138\delta^3 - 1.614\delta^4 + 0.502\delta^5.$$

Tonehole			
δ	t/b	Description	$t_a^{(o)}$ [mm]
0.66	0.48	FEM	0.78
		Keefe	0.8±0.2
		Eq. 14	0.84
		Eq. 15	0.70
		Eq. 16	0.93
		Eq. 17	0.78
0.32	3.15	FEM	0.000019
		Keefe	not measurable
		Eq. 14	0.000024
		Eq. 15	0.000018
		Eq. 16	0.000021
		Eq. 17	0.000021

Table 4: Series length correction $t_a^{(o)}$ in mm. Comparison between simulation, theories and experimental data for the toneholes studied by Keefe.

The open shunt impedance as a function of frequency is then evaluated as:

$$\overline{Z}_s^{(o)} = j \tan kt_e, \tag{35}$$

which, in the low frequency limit, becomes $\overline{Z}_s^{(o)} = jkt_s^{(o)}$. This expression works relatively well when $ka < 0.2$. More work is required to develop a formula that matches the simulation data up to $ka = 1$.

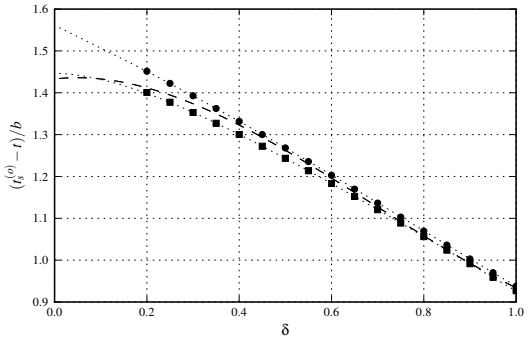

Figure 4: Difference between the shunt length correction $t_s^{(o)}$ and the tonehole height t divided by the tonehole radius b as a function of δ: FEM results for tall (squares) and short (circle) toneholes. Data fit formula (dotted). Current theory with Eq. 6 (dashed).

In Fig. 4, the simulation results are shown for the two extreme cases of short (circles) and tall (squares) toneholes as well as the data-fit formula (dotted) and the theoretical Eq. 6. This figure shows the sum of the radiation length correction and the inner length correction. As expected, for the toneholes of short height, this length correction is larger than for tall toneholes, because the unflanged tonehole ending becomes gradually "flanged" by the body of the instrument. Even for the tonehole of larger height, the new data-fit formula does not match exactly with the current theory, suggesting that the inner length correction found with our simulation is different. We can obtain the inner length correction t_i by subtracting the unflanged pipe radiation length correction $t_r = 0.6133b$ and the matching volume length correction t_m, Eq. 7, from Eq. 34 with $t \to \infty$:

$$t_i/b = 0.822 - 0.095\delta - 1.566\delta^2 + 2.138\delta^3 - 1.640\delta^4 + 0.502\delta^5. \tag{36}$$

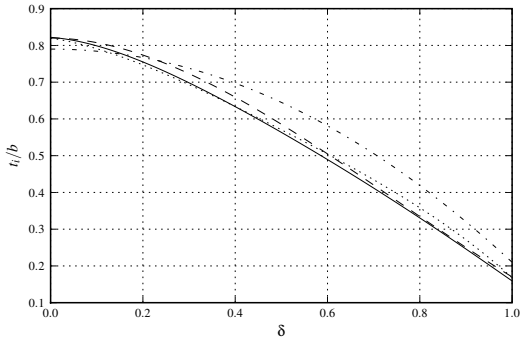

Figure 5: Comparison of Eq. 36 (solid curve) for the inner length correction $t_i^{(o)}/b$ with equations from the literature: Eq. 19 (dash-dot), Eq. 20 (dashed), Eq. 21 (dotted).

This formula is compared with the formulas from the literature in Fig. 5.

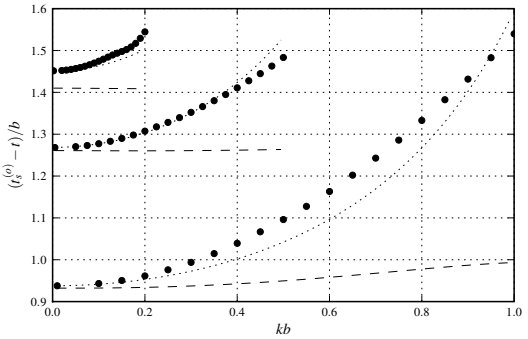

Figure 6: Difference between the shunt length correction $t_s^{(o)}$ and the tonehole height t divided by the tonehole radius b as a function of kb for three values of δ (0.2, 0.5 and 1.0, from top curve to bottom curve) and a value of $t/b = 0.1$ obtained from FEM simulations (filled circles). Current theory with Eq. 6 (dashed), new results with Eq. 35 (dotted).

The most important discrepancy between current tonehole theories and our simulation results concerns the frequency dependence of the shunt length correction for toneholes of short height, which is displayed in Fig. 6 for three toneholes with $t/b = 0.1$: (1) $\delta = 0.2$, (2) $\delta = 0.5$ and (3) $\delta = 1.0$. For each of these toneholes, the shunt length correction increases with frequency more than predicted. Equation 35 from this paper better predicts the frequency dependence compared to current theory but discrepancies remain. Similar results were obtained by Keefe (1982a) (see Fig. 3). One consequence of this behavior is that the higher resonances of an instrument with short chimney height are lower in frequencies than predicted by the current theory. This effect tends to shrink the ratio of higher resonances relative to the fundamental. For conical instruments, this counteracts the natural spreading of the resonances that occurs in truncated cones.

For the low frequency value of the series length correction, we obtained the following data-fit formula:

$$t_a^{(o)}/b\delta^4 = -f(\delta, t/b)g(\delta), \tag{37}$$

where

$$f(t/b) = 1 + (0.333 - 0.138\delta)\Big[1 - \tanh(2.666t/b)\Big],$$

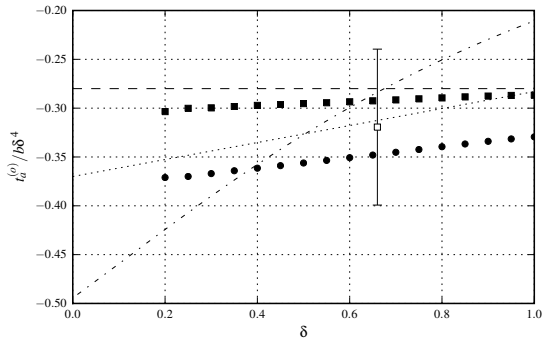

Figure 7: Series length correction $t_a^{(o)}/b\delta^4$ as a function of δ. FEM results: limit for large t/b (filled squares), limit for small t/b (filled circles). Theoretical formulas: Eq. 14 (dash-dot), Eq. 15 (dashed) and Eq. 16 (dotted).

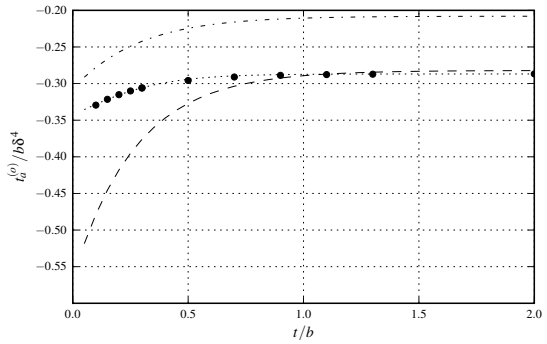

Figure 8: Series length correction $t_a^{(o)}/b\delta^4$ as a function of t/b for $\delta = 1.0$. FEM results (filled circles). Data fit formula Eq. 37 (dotted). Theory: Eq. 16 (dashed), Eq. 14 (dash-dot).

and

$$g(\delta) = 0.307 - 0.022\delta - 0.002\delta^2.$$

Figure 7 displays the results of our simulations for two extreme cases: short chimney height (circles) and large chimney height (squares), in comparison to theoretical formulas from the literature and an experimental data point from Keefe (1982a). This figure reveals that none of the theoretical equations is valid for all values of δ and chimney height. In the case of large chimney height, Eq. 15 provides a good approximation. The dependence of the series length correction on the tonehole height is displayed in Fig. 8 for a tonehole with $\delta = 1.0$, which reveals that neither Eq. 16 nor Eq. 14 match our FEM results.

The results of our simulations for closed toneholes confirm the validity of the low frequency limit of the shunt length correction. Figure 9 shows that the low frequency value of the shunt length correction is very well represented by the length $t + t_m$, that is, by the volume of the tonehole. The cotangent term in Eq. 13 tends toward infinity when $k(t + t_m) \to 0$, consequently, the influence of an inner length correction is expected to be maximal when $k(t + t_m) \approx \pi/2$ and negligible when it goes toward zero. As an example, for a tonehole height of 5 mm, the maximal influence of the inner length correction is above 20 kHz whereas, for a tonehole of 5 cm chimney height, this occurs above 2 kHz. Therefore, this term has a negligible influence even in the higher frequency range of woodwind instruments except possibly for instruments with very tall toneholes such as the bassoon (for which t varies between 5 to 40 mm). Nevertheless, to study this term, it is useful to define the impedance of the closed side hole

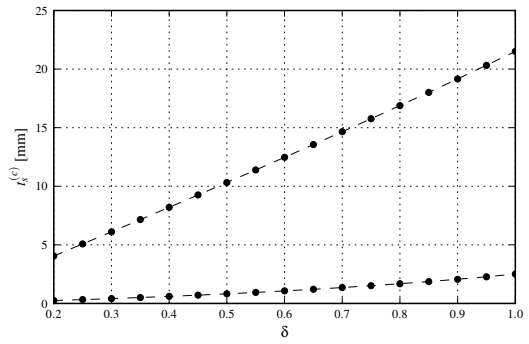

Figure 9: Shunt length correction $t_s^{(c)}$ as a function of δ with $t/b = 0.1$ (bottom) and $t/b = 2.0$ (top). FEM results (filled circles). Theoretical value $(t + t_m)$ where t_m is calculated using Eq. 7 (dashed).

as:

$$\overline{Z}_s^{(c)} = -j\cot k(t + t_m + t_i^{(c)}), \tag{38}$$

where t_m is the matching volume length correction defined in Eq. 7 and $t_i^{(c)}$ is the inner length correction (located inside the cotangent term rather than outside, thus it is not equivalent to the value from the literature). We can obtain the value of $t_i^{(c)}$ from our simulation results with:

$$t_i^{(c)} = \frac{1}{k}\tan^{-1}\left(\frac{1}{jZ_s^{(c)}}\right) - t - t_m. \tag{39}$$

This value may be compared with the current theoretical values by applying the previous equation to the calculated impedance of the closed side hole using Eq. 13. This is shown in Fig. 10. Discrepancies between the simulation results and the theoretical values exists. In the case of the short-height tonehole (top graph), the magnitude of the inner length correction is very small but it is remarkable that its value is negative for the two larger-diameter toneholes (δ values of 0.8 and 1.0). Discrepancies are also apparent for the large-height tonehole (bottom graph). In this case, the discrepancies are also most important for the larger-diameter toneholes. Further research is required to fully characterize this effect. For instruments with normally sized toneholes (flutes, clarinets, saxophones) this is likely negligible as explained previously.

In the case of the series length correction, we obtained a new formula that takes into account more precisely the height and radius of the toneholes:

$$\frac{t_a^{(c)}}{b\delta^4} = -f(\delta, t/b)g(\delta), \tag{40}$$

where

$$f(\delta, t/b) = 1 - [0.923 - 0.363\delta][1 - \tanh(2.385t/b)],$$

$$g(\delta) = 0.302 - 0.019\delta + 0.003\delta^2.$$

In Fig. 11, we consider the low frequency limit of the series length correction $t_a^{(c)}$ for short and tall tonehole heights compared to previous theories. The results for the tall tonehole are the same as for an open hole (see Fig. 7). When the toneholes are short in height, the series length correction term diminishes in magnitude. Figure 12 present this length correction as a function of the ratio t/b for one tonehole ($\delta = 1.0$) in comparison with current theories.

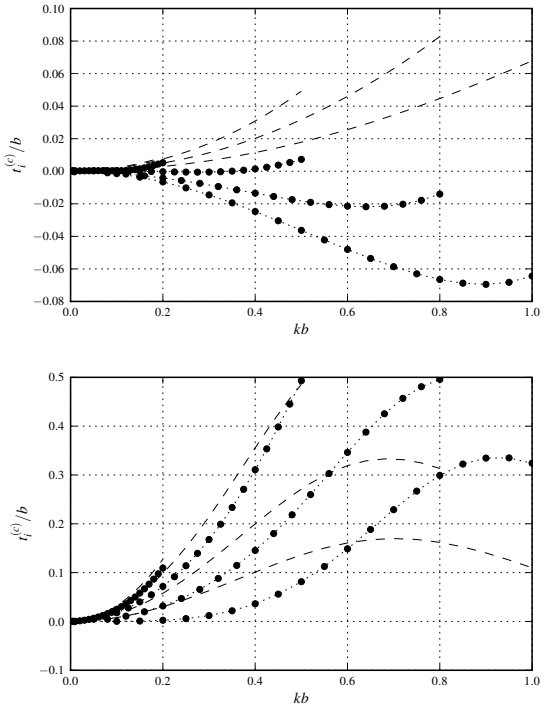

Figure 10: Inner length correction $t_i^{(c)}/b$ for closed toneholes as a function of kb for $\delta = 0.2, 0.5, 0.8, 1.0$ obtained from FEM simulations (filled circles) compared to theory (dashed). Top: $t/b = 0.5$, bottom: $t/b = 2.0$. The dotted line is a visual aid.

Impact of Conicity

A tonehole on a conical bore is no longer symmetric. In this situation, we propose to modify the model represented by Eq. 4 with:

$$\mathbf{T}_{hole} = \begin{bmatrix} 1+\overline{Z}_{a_u}/\overline{Z}_s & \overline{Z}_{a_u}+\overline{Z}_{a_d}+\overline{Z}_{a_u}\overline{Z}_{a_d}/\overline{Z}_s \\ 1/\overline{Z}_s & 1+\overline{Z}_{a_d}/\overline{Z}_s \end{bmatrix}, \qquad (41)$$

where $\overline{Z}_{a_u}$ is the series impedance for the upstream half of the tonehole and $\overline{Z}_{a_d}$ of the downstream half.

In a similar manner as for toneholes on cylindrical bores, we obtained the TM of the tonehole on a conical bore using Finite Element simulations. The transmission matrix $\mathbf{T}_{hole}$ of the tonehole is obtained from the transmission matrix $\mathbf{T}$ of the simulated system by multiplying this matrix by the inverse of the TM of the two segments of truncated cones, $\mathbf{T}_{cone_u}$ and $\mathbf{T}_{cone_d}$:

$$\mathbf{T}_{hole} = \mathbf{T}_{cone_u}^{-1}\mathbf{T}\mathbf{T}_{cone_d}^{-1}, \qquad (42)$$

where the TM of a conical waveguide is (Fletcher and Rossing 2008):

$$\mathbf{T}_{cone} = \begin{bmatrix} -rt_{out}\sin(kL-\theta_{out}) & jr\sin kL \\ jrt_{in}t_{out}\sin(kL-\theta_{out}+\theta_{int}) & rt_{in}\sin(kL+\theta_{in}) \end{bmatrix}, \qquad (43)$$

where x_{in} and x_{out} are respectively the distances of the input plane and output plane from the apex of the conical frustum and where $r = x_{out}/x_{in}$, $L = x_{out} - x_{in}$, $\theta_{in} = \arctan(kx_{in})$, $\theta_{out} = \arctan(kx_{out})$, $t_{in} = 1/\sin\theta_{in}$ and $t_{out} = 1/\sin\theta_{out}$.

We are interested in determining whether or not the shunt impedance $\overline{Z}_s$ is different from that derived for a cylindrical bore and to determine the effect of the asymmetry on the values of $\overline{Z}_{a_u}$ and $\overline{Z}_{a_d}$. The tonehole parameters were obtained for two conical waveguides with taper angles of 3 and 6 degrees. As

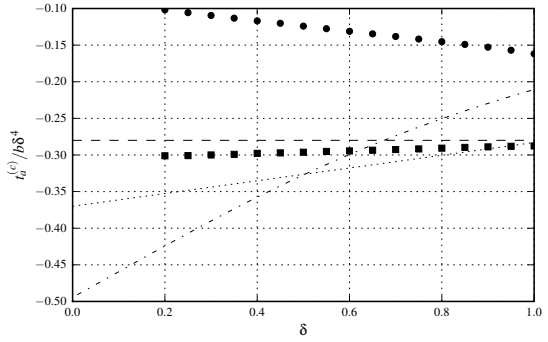

Figure 11: Series length correction $t_a^{(c)}/b\delta^4$ as a function of δ. FEM results: limit for large t/b (filled squares), limit for small t/b (filled circles). Theoretical formulas: Eq. 14 (dash-dot), Eq. 15 (dashed) and Eq. 16 (dotted).

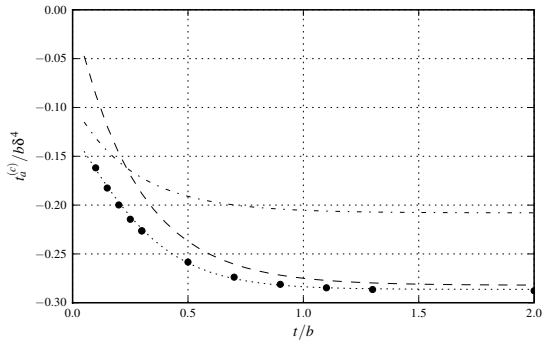

Figure 12: Series length correction $t_a^{(c)}/b\delta^4$ as a function of t/b for $\delta = 1.0$. FEM results (filled circles). Data fit formula Eq. 37 (dotted). Theory: Eq. 16 (dash-dot), Eq. 14 (dashed).

for toneholes on a cylindrical bore, we developed a data-fit formula for the shunt equivalent length of the open tonehole from the simulation data (with the same set of parameters). Then we calculated the differences between the two fit formulae and determined that the maximal difference is $4 \times 10^{-5}\, b$ in both cases. This is a very small difference and we are confident to conclude that the shunt length corrections are unchanged relative to their values on a cylindrical bore.

A conclusion for the series length correction is more difficult. For the simulations of toneholes on cylindrical bores, we solved only half the system, thus forcing the symmetry. In the case of the conical bore, the complete system is solved and the TM is not forced to be symmetric, which seems to augment numerical errors. As can be seen in Fig. 13, the upstream and downstream values of the series length correction are very close to one another even though they become slightly different for smaller values of δ. The impact of the series length correction being relatively small and increasingly less important as the toneholes become smaller, this is likely to be negligible.

From this analysis, we conclude that the use of TM parameters developed for toneholes on cylindrical bores are valid for conical bores, at least up to an angle of 6 degrees and probably for wider angles as well.

CONCLUDING REMARKS

We obtained new formulas for the shunt and series impedance of an unflanged tonehole that is valid for tonehole heights com-

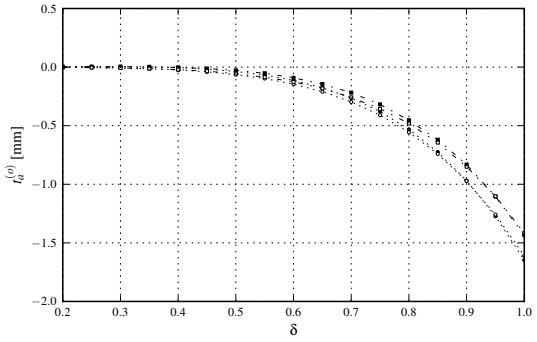

Figure 13: Series length correction t_a in mm for a tonehole on a conical bore with taper angle of 3 degrees: limit for long (squares) and short (circles) toneholes – upstream part (filled), downstream part (unfilled).

mon in woodwind instruments. For an open tonehole, the shunt length correction is expressed in Eq. 34 and the series length correction in Eq. 37. For a closed side hole, the series length correction is expressed in Eq. 40 whereas the shunt length correction from the literature, Eqs. 11 and 12, are valid.

We verified that the shunt length correction of a tonehole on a cylindrical bore can be used as well on a conical bore.

ACKNOWLEDGEMENTS

The authors would like to thank Jean-Pierre Dalmont for providing experimental results. They also wish to acknowledge the support of the Natural Sciences and Engineering Research Council of Canada, the Canadian Foundation for Innovation, and the Centre for Interdisciplinary Research in Music Media and Technology at McGill University. The first author gratefully acknowledges the Fonds Québécois de la Recherche sur la Nature et les Technologies for a doctoral research scholarship.

REFERENCES

Dalmont, Jean-Pierre et al. (2002). “Experimental Determination of the Equivalent Circuit of an Open Side Hole: Linear and Non Linear Behaviour”. *Acustica* 88, pp. 567–575.

Dubos, V. et al. (1999a). “Theory of Sound Propagation in a Duct with a Branched Tube Using Modal Decomposition”. *Acustica* 85, pp. 153–169.

Dubos, Vincent et al. (1999b). “Theory of Sound Propagation in a Duct with a Branched Tube Using Modal Decomposition”. *Acustica* 85, pp. 153–169.

Fletcher, Neville H. and Thomas D. Rossing (2008). *The Physics of Musical Instruments*. 2nd ed. 1998. Springer.

Keefe, Douglas H. (1981). “Woodwind Tone Hole Acoustics and the Spectrum Transformation Function.” PhD thesis. Case Western Reserve University.

— (1982a). “Experiments on the single woodwind tonehole”. *J. Acoust. Soc. Am.* 72.3, pp. 688–699.

— (1982b). “Theory of the single woodwind tonehole”. *J. Acoust. Soc. Am.* 72.3, pp. 676–687.

— (1990). “Woodwind air column models”. *J. Acoust. Soc. Am.* 88, pp. 35–51.

Nederveen, C. J. et al. (1998). “Corrections for Woodwind Tone-Hole Calculations”. *Acustica* 84, pp. 957–966.

Nederveen, Cornelis Johannes (1998). *Acoustical Aspects of Woodwind Instruments*. Revised. DeKalb, Illinois: Northern Illinois University Press, p. 147.

Pierce, Allan D. (1989). *Acoustics, An Introduction to Its Physical Principles and Applications*. Woodbury, New-York: Acoustical Society of America, p. 678.